CHEMISTRY
A EUROPEAN JOURNAL

DOI: 10.1002/chem.200600349

Synthesis of Size-Controlled Acid-Resistant Hybrid Calcium Carbonate Microparticles as Templates for Fabricating "Micelles-Enhanced" Polyelectrolyte Capsules by the LBL Technique

Xiaodong Li,[a] Qiaoling Hu,*[a] Linhai Yue,[b] and Jiacong Shen[a]

Abstract: Size-controlled, low-dispersed calcium carbonate microparticles were synthesized in the presence of the amphiphilic block copolymer polystyrene-*b*-poly(acrylic acid) (PS-*b*-PAA) by modulating the concentration of block copolymer in the reactive system. This type of hybrid microparticles have acid-resistant properties. By investigating the aggregation behaviors of PS-*b*-PAA micelles by transmission electron microscopy (TEM), the mechanism of hybrid calcium carbonate formation illustrated that the block copolymer served not only as "pseudonuclei" for the growth of calcium carbonate nanocrystals, but also forms the supramicelle congeries, a spherical framework, as templates for calcium carbonate nanocrystal growth into hybrid $CaCO_3$ particles. Moreover, this pilot study shows that the hybrid microparticle is a novel candidate as a template for fabricating multilayer polyelectrolyte capsules, in which the block copolymer is retained within the capsule interior after core removal under soft conditions. This not only facilitates the encapsulation of special materials, but also provides "micelles-enhanced" polyelectrolyte capsules.

Keywords: acid resistance · block copolymers · crystal growth · layer-by-layer technique · micelles

Introduction

The deposition of polyelectrolyte multilayers has received much attention since the layer-by-layer technique was introduced by Decher in 1997.[1] Through application to the coating of colloidal particles and the subsequent dissolution of the template, this procedure leads to the formation of hollow microcapsules.[2] More attention has been paid to this method due to its potential application in the fields of drug delivery, biosensors, microreactors, and bioseparations.[3] A wide variety of substrates with charged surfaces has been used as templates for formation of multilayer capsules, such as weakly cross-linked melamine formaldehyde (MF) latices, organic and inorganic crystals, silica particles, polystyrene latices, metal nanoparticles and nanorods, and biological templates. Each of these has its own advantages and limitations.[2a,4]

It is commonly believed that perfect templates must fulfil three requirements: stability in the layer-by-layer (LBL) process, the condition of core disposal not affecting the structure and stability of the multilayer, and no residue of dissolved template.[5] In fact, the means of template decomposition has an important effect on the properties of polyelectrolyte capsules. Organic templates of artificial polymers, such as MF and polystyrene (PS), need harsh conditions to remove the core, such as strong acids or organic solvents. At the same time, it is difficult to completely dispose of the core from the hollow capsules, due to interactions with the capsule wall. Silica dioxide particles are a promising alternative as templates, as there is no swelling of the integrated capsules and no core residue within the capsules. However, hydrofluoric acid is needed in the process of silica dioxide particle dissolution. Recently, the use of inorganic crystals, such as $CdCO_3$, $CaCO_3$, and $MnCO_3$, has been reported. These can be prepared with low distribution by rather simple methods and serve as templates.[6] The core can be disposed of under mild conditions and the products can completely leave the capsule without problem. Hollow capsules would be obtained. However, all of the available templates served as a physical support only, and the struc-

[a] Dr. X. Li, Prof. Dr. Q. Hu, Prof. Dr. J. Shen
Institute of Polymer Composites, Zhejiang University
38 Zheda Road, Hangzhou 310027 (China)
Fax: (+86) 571-8795-3726
E-mail: huql@zju.edu.cn

[b] Prof. Dr. L. Yue
Chemistry Department, Zhejiang University
38 Zheda Road, Hangzhou 310027 (China)

Supporting information for this article is available on the WWW under http://www.chemeurj.org/ or from the author.

ture of the resultant polyelectrolyte (PE) capsules wall is loose and porous. In addition, the high permeability of the polyelectrolyte shell, leading to the low encapsulation efficiency and high speed of release,[7] made it difficult for these hollow capsules to be used in practice. Efforts are being made to find novel templates for desirable hollow capsules.[5]

Many efforts have been made to synthesize hybrid organic–inorganic microparticles with controlled size distribution and controlled morphology, due to their broad applications in scientific and technological domains.[8] Some hybrid microparticles were synthesized in the presence of, for example, linear amphiphilic polymeric additives or dendrimers.[9] Properties, such as morphology, ξ-potential, and the crystal type of the microparticles, are strongly affected by the organic additives. So far, more attention has been paid to hybrid-complex preparation than to the potential applications of these hybrid complexes. Actually some of these microparticles, such as hybrid calcium carbonate, can serve as templates for fabricating polyelectrolyte microcapsules by the layer-by-layer technique. In contrast to conventional templates, if these hybrid microparticles serve as templates to fabricate polyelectrolyte capsules, the core cannot be completely dissolved because of the large molecular weight and/or charge properties of organic additives in the formation of the hybrid particles. If certain organic additives retained inside the capsules interact with and reconstruct the capsule wall, the structure of the conventional PE capsules will be changed.

Here, we report a novel technique for the preparation of size-controlled hybrid calcium carbonate microparticles in the presence of polystyrene-*b*-poly(acrylic acid) (PS-*b*-PAA), an amphiphilic block copolymer that can be used as a template for fabricating polyelectrolyte capsules. PS-*b*-PAA was selected to control the morphology and particle size of the hybrid calcium carbonate complex. The negatively charged microparticles with tunable diameters of 1–10 μm were successfully prepared by simply modulating the concentration of PS-*b*-PAA in the reactive system. Interestingly, this kind of hybrid microparticle exhibits acid-resistant properties, even in strong acid solution. We found that the mechanism of hybrid particle formation is responsible for the special acid-resistant properties. In addition, we provide evidence that these acid-resistant hybrid calcium carbonate microparticles can serve as templates to fabricate polyelectrolyte microcapsules by the LBL technique, and the templates can be removed under soft conditions. A novel capsule enhanced by PS-*b*-PAA-based micelles was obtained.

Results and Discussion

Characterization of hybrid $CaCO_3$ microparticles: Three batches of microparticles were prepared (see Experimental Section) and were named batches A, B, and C according to the initial concentration of PS-*b*-PAA in the reaction system; 0.24, 0.64, and 1.28 mM, respectively. The surface morphology of these hybrid microparticles was examined by scanning electron microscopy (SEM) (Figure 1a–c). These hybrid particles have compact surfaces, in contrast to previous reports.[4a] The three batches examined (A, B, C) have low size distribution, and whatever the size of the hybrid particles, they have similar morphology. The coulter LS-230 laser particle-size analyzer was used to measure directly the size and size distribution of the hybrid calcium carbonate microparticles. The size measurements were consistent with the SEM results. The size distribution of the three batches A–C is low, the mean particle sizes are 8.29 ± 0.51, 4.16 ± 0.39, and 1.78 ± 0.37 μm, respectively, as shown in Figure 1d.

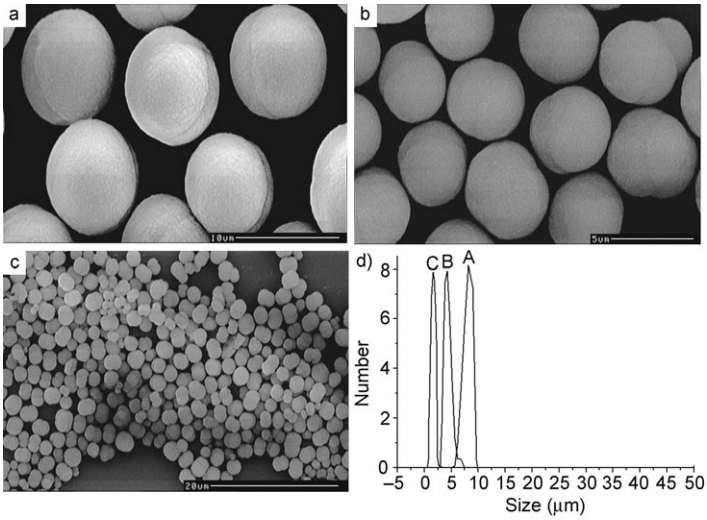

Figure 1. SEM images of hybrid calcium carbonate microparticles in the presence of different initial concentrations of block copolymer PS-*b*-PAA: a) 0.24 mM batch A (scale bar represents 10 μm), b) 0.64 mM batch B (scale bar represents 5 μm), c) 1.28 mM batch C (scale bar represents 20 μm). d) Corresponding size distribution of the three batches.

The thermogravimetric analysis (TGA) curve was used to determine the content of block copolymer in the hybrid microparticles of batches A–C. These results indicate that more than 10% polymer (10, 12, and 15% for A, B, and C, respectively) was contained in the hybrid microparticles, as shown in Figure 2a (the weight loss at temperatures lower than 200°C was thought to be due to the water content in the hybrid microparticles). X-ray diffraction (XRD) was used to determine the type of crystal-forming microparticles before and after heating in a muffle furnace for 2 h (Figure 2b). It is clear that all the reflections can be readily indexed to a pure calcite phase of $CaCO_3$ conforming to a space group of *R*3*c* (167) (JCPDS 851108). It is also apparent that the type of $CaCO_3$ nanocrystals forming microparticles before and after treatment is complete calcite.

By modulating the concentration in the initial reaction system, hybrid calcium carbonate microparticles of different sizes were formed by the procedure mentioned above. The result of size measurement is shown in Figure 3. By considering the relationship between the particle size and the ini-

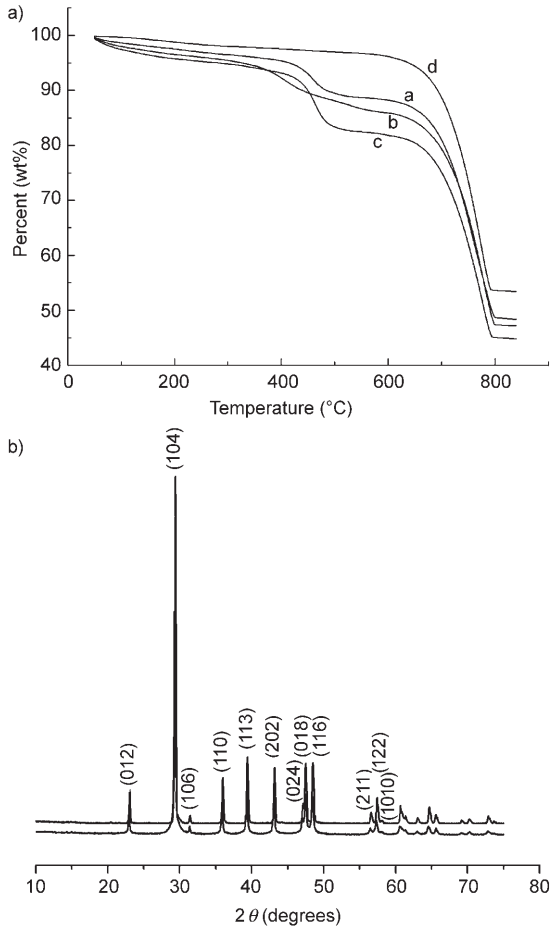

Figure 2. a) TGA curves of calcium carbonate and hybrid calcium carbonate microparticles in the presence of different initial PS-*b*-PAA concentrations: a) 0.24 mM batch A, b) 0.64 mM batch B, c) 1.28 mM batch C, d) 0 mM. The PS-*b*-PAA content in batches A, B, and C is about 10, 12, and 15%, respectively. b) XRD patterns of batch A: lower trace, before heating; upper trace, after heating for 2 h at 550°C in a N_2 atmosphere in a muffle furnace.

tial concentration of copolymer in the reaction system, it could be concluded that as the PS-*b*-PAA concentration increased, the size of hybrid calcium carbonate microparticles obtained decreased. By altering the concentration of block copolymer in the reaction system, the size of the hybrid calcium carbonate microparticles ranging from 1–10 μm can be modulated. Surprisingly, this kind of hybrid calcium carbonate particles could not dissolve in an acidic aqueous solution, such as 0.1 M hydrochloric or sulfuric acid, or even in 0.1 M disodium-EDTA solution (pH≈4.50, determined by pH meter).

Acid-resistance analysis of hybrid microparticles: Three samples (0.5 g each) of hybrid microparticles from batch A (initial concentration of PS-*b*-PAA, 0.24 mM) were immersed in 50 mL of 0.1 M hydrochloric acid, sulfuric acid, and disodium-EDTA solution, respectively, for one day. Confocal laser scanning microscopy (CLSM) was used to observe the morphology of the hybrid microparticles in the

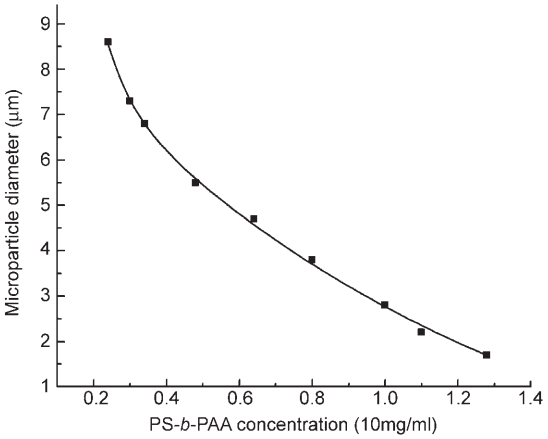

Figure 3. Relationship between particle diameter and initial concentration of block copolymer PS-*b*-PAA in the reaction system.

different solutions. The images shown in Figure 4 suggest that hybrid microparticles have acid-resistant properties. Hybrid microparticles treated with hydrochloric acid and

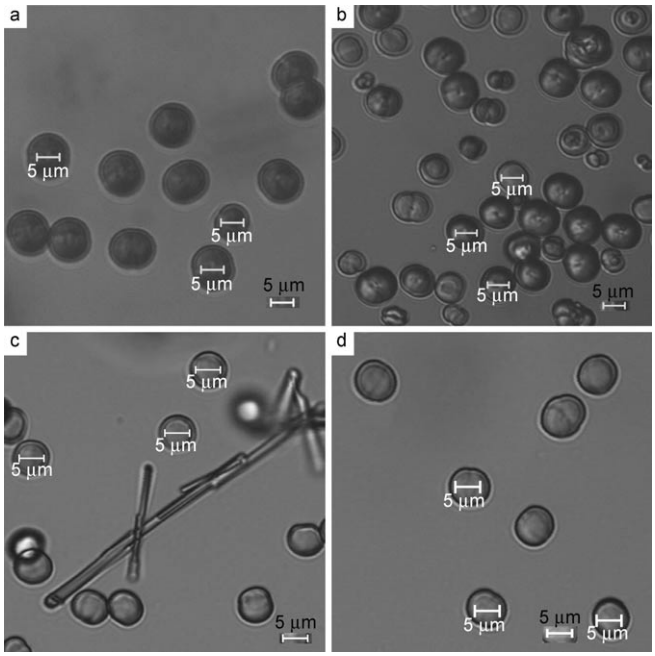

Figure 4. CLSM images of hybrid microparticles of batch A (initial concentration of PS-*b*-PAA, 0.24 mM). a) untreated; b) treated with 0.1 M HCl; c) treated with 0.1 M H_2SO_4; d) treated with 0.1 M disodium-EDTA solution. Treatment time was 24 h. Scale bars represent 5 μm.

disodium-EDTA solution have similar morphologies to untreated hybrid microparticles (Figure 4a, b, d). In contrast, hybrid microparticles treated with sulfuric acid appeared different (Figure 4c). New needlelike substances appeared in the sulfuric acid solution. In addition, the samples treated with disodium-EDTA and sulfuric acid varied to some extent, whereas samples treated with hydrochloric acid changed little. X-ray diffraction (XRD) was used to analyze

the crystal types (Figure S1). The crystal type of hybrid microparticles treated with hydrochloric acid and disodium-EDTA was still calcite (Figure S1a, c), the same as that of the untreated samples, whereas calcium sulfate crystals appeared in the sample treated with sulfuric acid. FTIR spectra showed that samples treated with hydrochloric acid and disodium-EDTA have the same components (Figure S2a, b, d), whereas calcium sulfate was detected in the sample treated with sulfuric acid (Figure S2c). The size and components of the samples treated under different conditions remained almost unchanged after one day (data not shown). Clearly, hybrid microparticles have strongly acid-resistant properties in contrast with pure calcium carbonate. By taking the method of synthesis of hybrid particles into consideration, the presence of block copolymer in the hybrid particles should account for these special properties.

The mechanism of formation of hybrid $CaCO_3$ particles: PS-*b*-PAA is an amphiphilic copolymer that can form micelles in aqueous solution if the concentration is above the critical micelle concentration (CMC). In our initial reactive system, the PS-*b*-PAA concentration is far above its CMC ($0.006\ g\,L^{-1}$). In addition, the PAA segment of the block copolymer is in its ionized form in basic sodium carbonate solution. This suggests that micelles with PS hydrophobic cores and PAA hydrophilic shells assemble in these cases. This type of micelle is dynamically stable in aqueous solution, due to the glass nature of the PS segment.[11] Furthermore, the individual micelle can form intermicellar aggregates through the "bridge effect" of calcium ions, which has been also reported by Eisenberg and co-workers.[11]

Transmission electron microscopy (TEM) was used to study how the Ca^{2+} ions interact with the block-copolymer-based micelles in basic aqueous solution, as shown in Figure 5. These results indicate that Ca^{2+} ions can bridge the micelle to form a copolymer/Ca^{2+} complex, a large, irregular, networklike supramicelle congeries. Copolymer solutions of 0.4, 0.6, 0.8, and 1 wt% were investigated by TEM as well. The results are similar to that of 0.2% copolymer solution (data not shown).

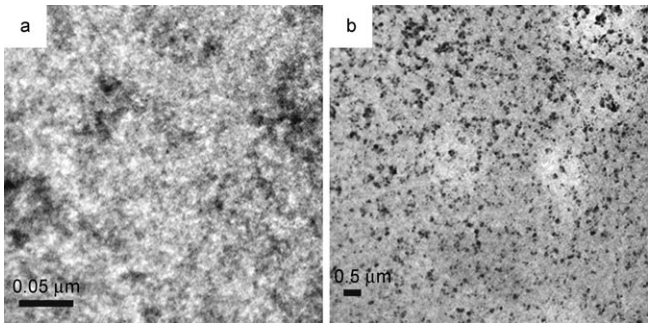

Figure 5. TEM images of the morphology of block copolymer aggregates in 500 μL PS-*b*-PAA copolymer solution (block copolymer concentration 0.2% (w/w), copolymer was dissolved in 1% (wt%) ammonia). a) In the presence of 5 μL 1 mM $CaCl_2$ solution. b) No $CaCl_2$ solution.

Information about the influence of copolymer on the formation of the hybrid calcium carbonate microparticles was also provided by TEM. As shown in Figure 6, the morphology of copolymer aggregates changed as the amount of copolymer introduced into the reaction system gradually increased. The morphology of the sample without calcium chloride (Figure 6a) differs from the morphology of the sample with 5 μL calcium chloride (Figure 6b). Ca^{2+} ions worked not only as precipitator to produce $CaCO_3$ crystals, but also as bridging agent to form micelle congeries, due to the interaction of Ca^{2+} ions with carboxylic acid groups in the PAA segments. As for the sample with 15 μL calcium chloride, an interesting phenomenon was found, as shown in Figure 6c. The copolymer formed a spherical-shaped network. The inset image in Figure 6c clearly indicates that cal-

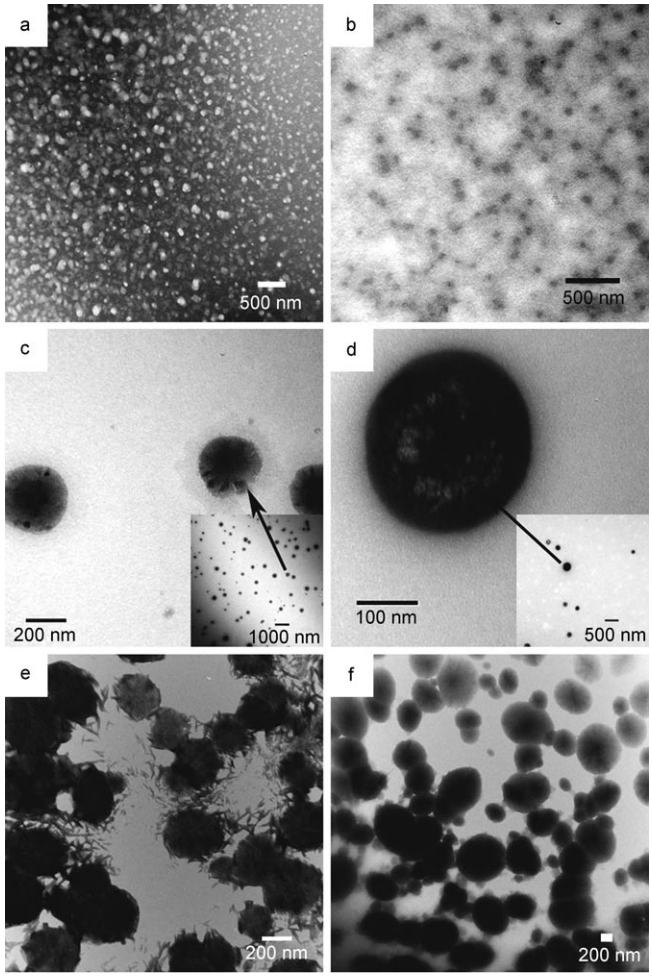

Figure 6. TEM images of the morphology of block copolymer aggregates in 500 μL block copolymer Na_2CO_3 solution (block copolymer concentration 0.8 mM, concentration of sodium carbonate 0.2 mM). a) No $CaCl_2$ solution. b) In the presence of 5 μL $CaCl_2$ solution. c) In the presence of 15 μL $CaCl_2$ solution, low-magnification image in inset. d) In the presence of 30 μL $CaCl_2$ solution, low-magnification image in inset. e) Sample (c) aged for two weeks. f) Sample (d) aged for two weeks.

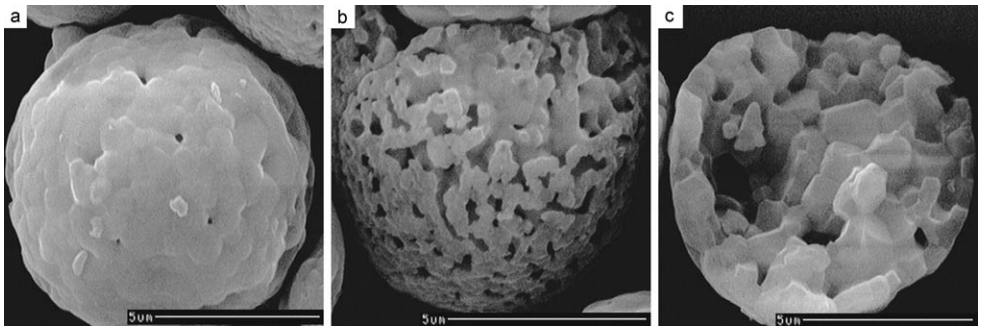

Figure 7. a) SEM image of hybrid calcium carbonate microparticles heated at 10 °C per minute to 550 °C and calcined at 550 °C in N_2 atmosphere for 20 min. b,c) SEM images of the surface and section, respectively, of hybrid calcium carbonate microparticles treated for 60 min. Scale bars represent 5 μm.

cium carbonate nanocrystals grow in the network (indicated by the arrow). The case of the sample with 30 μL calcium chloride is similar to that of the sample with 15 μL calcium chloride, although the amount of calcium carbonate in the network was more than that of the sample with 15 μL calcium chloride (Figure 6d). These results suggest that PS-*b*-PAA formed supramicelle congeries, spherical-shaped networks in the presence of Ca^{2+} ions, in which calcium carbonate nanocrystals grow. TEM images of specimens kept at 4 °C for two weeks indicate that the structure of the spherical-shaped network is fairly stable (Figure 6e, f). In considering 10–15 % copolymer content in the hybrid microparticles, it is speculated that block-copolymer-based micelles work as "pseudonuclei" for the formation of calcium carbonate nanocrystals nuclei, and also that the supramicelle congeries can form spherical frameworks for $CaCO_3$ nanocrystals growth. The nanocrystals linked with one another in this kind of network eventually led to the formation of hybrid microparticles. This process is similar to the synthesis of calcium carbonate in hard tissues of organisms—the inorganic crystals grow directionally in the organic templates, and the organic content in the product is much lower than the inorganic content.[12]

Microspheres from batch A (initial concentration of PS-*b*-PAA, 0.24 mM) were calcined in a muffle furnace at 550 °C, at which the weight of the organic composition was lost completely, as shown in the TGA curve (Figure 2a). As the temperature increased to 550 °C at 10 °C min^{-1} under the N_2 atmosphere, the block copolymer was completely removed from the hybrid particles. After 20 and 60 min, some of microparticles were removed for SEM investigation. As shown in Figure 7, the morphology of the specimen heated for 20 min was different to that of the unheated sample (Figure 7a). After 60 min, the morphology of the specimen changed further. The surface of the microparticles reveals many holes (Figure 7b). Inside the microparticles, many pieces of calcium carbonate nanocrystals were stacked into a microsphere (Figure 7c). If heated for more than 4 h, the microspheres lost its spherical shape and broke into several pieces. Furthermore, the heated particles were soluble in acidic solution. This result suggested that the PS-*b*-PAA block copolymer acts as a framework in the formation of hybrid calcium carbonate microparticles. Additionally, the block copolymer in hybrid microparticles is responsible for the acid-resistant properties of the hybrid microparticles.

The process of preparing hybrid microparticles is illustrated in Scheme 1. Firstly, the block copolymer is dissolved in

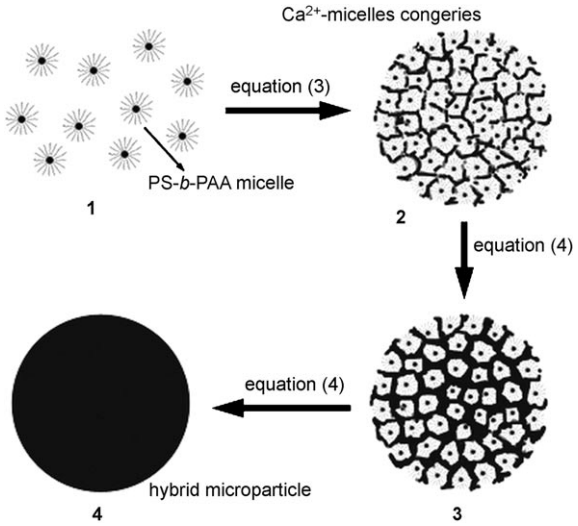

Scheme 1. Preparation of hybrid calcium carbonate microparticles in the presence of PS-*b*-PAA block copolymer. 1) Formation of PS-*b*-PAA-based micelles; 2) formation of supramicelle congeries; 3) PS-*b*-PAA-based micelle congeries not only as "pseudonuclei" to produce calcium carbonate nanocrystals, but also as templates to control calcium carbonate nanocrystal growth inside the network; 4) formation of hybrid calcium carbonate.

sodium carbonate solution to form micelles (1), then the micelles interact with Ca^{2+} ions to form micelle/Ca^{2+} congeries—the spherical-shaped network (2). These supramicelle congeries are stable and can be isolated in aqueous solution, unlike conventional micelles, due to two reasons: one is the glassy state of the PS chains at the reaction temperature,[11] the other is the bridging effect of the Ca^{2+} ions between different carboxylic groups of the PAA chains. The concentration of carboxylic groups inside the spherical-shaped micelle

congeries is much higher than that in the bulk of the reaction system. In addition, these micelle congeries have a huge surface area.[13] According to molecular-reaction dynamics,[14] the odds of interaction of Ca^{2+} ions with carboxylic groups in PAA are much greater than those for the interaction with carbonate in the bulk of system. As a result, the concentration of Ca^{2+} inside the congeries is much higher than that in the bulk solution. Thus, carbonate ions enter the interior of the supramicelle congeries, replacing the carboxylic group combined with Ca^{2+} ions to produce calcium carbonate. Nuclei of calcium carbonate are produced on the surface of the micelles in a particular direction. Once calcium carbonate crystal nuclei are formed, the micelles around the crystal in the spherical framework will interact with them in other directions and limit anisotropic crystal growth. As a result, many nanocrystal nuclei enwrapped by micelles grow within the congeries (step 3, Scheme 1). Finally, $CaCO_3$ nanocrystals form a hybrid calcium carbonate microsphere through a micelle–Ca^{2+} linkage (step 4, Scheme 1). The process is shown as the following reactive equations:

$$CO_3^{2-} + H_2O \rightleftharpoons HCO_3^- + OH^- \quad (1)$$

$$-COOH + OH^- \rightleftharpoons -COO^- + H_2O \quad (2)$$

$$Ca^{2+} + -COO^- \leftrightharpoons -COOCaOOC^- \quad (3)$$

$$-COOCaOOC^- + CO_3^{2-} \leftrightharpoons CaCO_3\downarrow + -COO^- \quad (4)$$

Clearly, PS-*b*-PAA-based micelle congeries serve not only as "pseudonuclei" to produce calcium carbonate nanocrystals, but also as templates to control calcium carbonate nanocrystal growth inside the network. Furthermore, the ζ-potential of the hybrid microparticles suggested highly negatively charged surfaces (Figure 8), which is different from that of pure calcium carbonate microparticles.[4d,6a] The PS-*b*-PAA-coated crystal surface is responsible for this result.

According to the formation mechanism, the micelle/Ca^{2+} complex should be responsible for acid-resistant properties. The results of the acid-resistance studies mentioned above confirm that the morphologies of hybrid particles treated with different solutions retained their spherical shape, although some of the $CaCO_3$ crystals of the microparticles dissolved in acidic solution. Presumably, the $CaCO_3$ nanocrystals within the hybrid-microparticle surface dissolved in acidic solution, and subsequently an organic layer was formed by the deposition of PS-*b*-PAA micelle/Ca^{2+} complexes on the hybrid microparticles provided a physical barrier to prevent further dissolution of remaining $CaCO_3$ crystals.

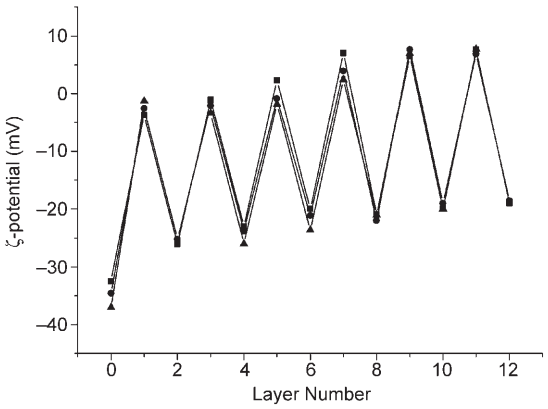

Figure 8. ζ-potential as a function of layer number for hybrid particles coated with alternately PAH (odd) and PSS (even) as the outer layer (PAH and PSS solutions 2 mg mL^{-1}, deposition time 10 min, 200 µL removed for ζ-potential detection). The lines are to guide the eye and have no physical meaning. -■- ξ-potential line of batch A; -●- ξ-potential line of batch B; -▲- ξ-potential line of batch C.

Further research of this acid-resistant mechanism is underway and will be reported in near future.

Fabrication multilayers on hybrid $CaCO_3$ particles: The surface potential of the hybrid particles is highly negatively charged (Figure 8). The first deposition layer is positively charged poly(allylamine hydrochloride) (PAH), and then negatively charged poly(styrene sulfonate sodium salt) (PSS) is deposited as a secondary layer. The ζ-potential curve changes upon the deposition of each layer of PAH/PSS pairs, indicating the successful layer-by-layer assembly of polyelectrolyte multilayers onto hybrid microparticles (Figure 8). After deposition of the desired number of (PAH/PSS) layers, the cores were removed. As described above, these hybrid cores cannot dissolve in acidic aqueous solutions, such as hydrochloric acid or even disodium-EDTA solution, due to their special formation mechanism. However, trisodium-EDTA solution (pH 7.28) can be used to remove the core, and polyelectrolyte capsules were obtained accordingly.

These polyelectrolyte capsules (PAH labeled with fluorescein isothiocyanate (FITC)) of the three batches A–C were

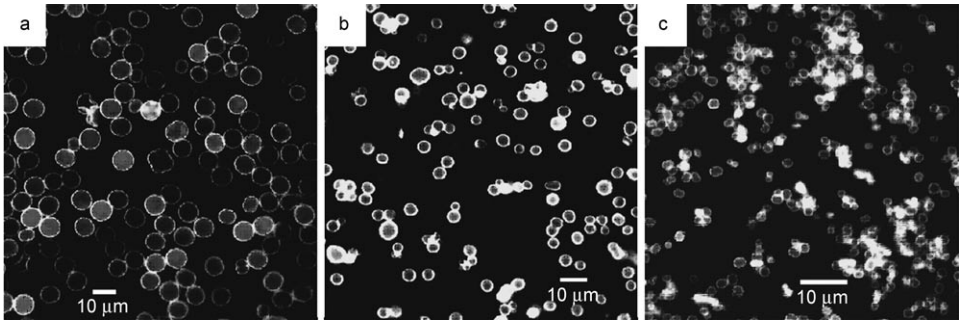

Figure 9. CLSM images of $(PAH/PSS)_6$ capsules on different hybrid particles. a) batch A, b) batch B, c) batch C. The images of batches A and B were collected by using a 40× objective, and the image of batch C was collected by using a 100× oil-immersion objective. PAH was labeled with FITC.

viewed by confocal microscopy. As shown in Figure 9, all three batches show low size distribution, efficiency of capsule formation, and integrity of microcapsules with nanoscale walls. SEM was employed to investigate the morphology of the dried hollow capsules, as shown in Figure 10. Images of the pure $CaCO_3$ capsules of six bilayers of (PSS/PAH)$_6$ have been reported to show a very porous network.[4-d,6a] This is in contrast to the images of the hybrid $CaCO_3$ capsules of six (PAH/PSS)$_6$ bilayers (Figure 10a, c). The structure of the capsule wall is different from that of the pure $CaCO_3$ capsule wall.

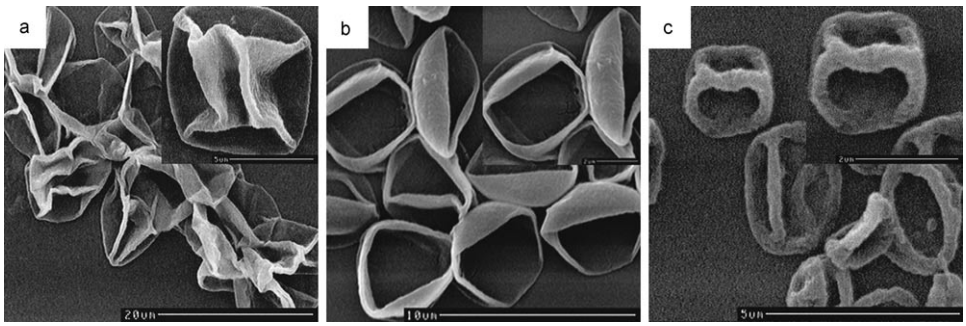

Figure 10. SEM images of (PAH/PSS)$_6$ capsules on different hybrid particles. Higher-magnification images are shown in the insets. a) Batch A: scale bar in main picture represents 20 μm; in inset, 5 μm. b) Batch B: scale bar in main picture represents 10 μm; in inset, 2 μm. c) Batch C: scale bar in main picture represents 5 μm; in inset, 2 μm.

Structure of the novel PE capsules containing micelles: The particular structure of the hybrid capsules derived from the block copolymer PS-*b*-PAA was retained inside the capsules. Field-emission scanning-electron microscopy (FESEM) with elemental analysis using energy-dispersive X-ray spectroscopy (GENENIS4000, EDAX) was used to investigate the fine structure of the hybrid polyelectrolyte capsules of batch A (initial concentration of PS-*b*-PAA, 0.24 mM, Figure 11). FESEM-EDX was used to detect the presence of calcium after the dissolution of the cores (Figure 11, top). Clearly, the presence of calcium is not detectable by EDX, as shown in the inset of Figure 11 (top). This indicates successful removal of the inorganic component in the hybrid templates (the detection limit of calcium ions for EDAX is 0.1 wt%). Figure 11 (bottom), also revealed that the wall of the hybrid polyelectrolyte capsule was a compact and thick membrane, in contrast to the porous network of polyelectrolyte capsules based on pure $CaCO_3$ particles reported previously. Additionally, there are many tiny protuberances on the surface of the capsules. It seems that many nanoparticles with a size of about 100 nm are inside the capsule.

As presented in Figure 12, the thickness of the hybrid polyelectrolyte capsule wall was 110 ± 20 nm (Figure 12, top). The thickness of each bilayer of the microcapsule has been reported to be about 5 nm.[15] The wall of the hybrid capsules is much thicker than that of the conventional polyelectrolyte capsules with the same six deposition layers (≈ 30 nm). Clearly, the block copolymer PS-*b*-PAA was left inside the capsule interior. By considering all of these results together, it is presumed that the block copolymer PS-*b*-PAA retained inside the capsule interior is in the form of micelles and/or micelle/Ca^{2+} complexes.

Further study revealed that the PS-*b*-PAA-based negatively charged micelles can interact with the PAH layer (Figure 13). It is likely that some or all of the PS-*b*-PAA-based micelles were involved in the formation of the capsule wall, leading to a thick and compact "micelles-enhanced" hybrid capsule wall. In addition, it has been verified that PS-*b*-PAA micelles can be stabilized and isolated in water in the presence of Ca^{2+} ions, forming supramicelle aggregates.[11] As a result, many negatively charged micelles retained inside the capsule produced a excess negative surface inside the polyelectrolyte capsule, which inevitably has a great effect on the encapsulation behaviors and release behaviors of this kind of capsule. The process of preparing micelles-enhanced capsules is detailed in Scheme 2. PE cap-

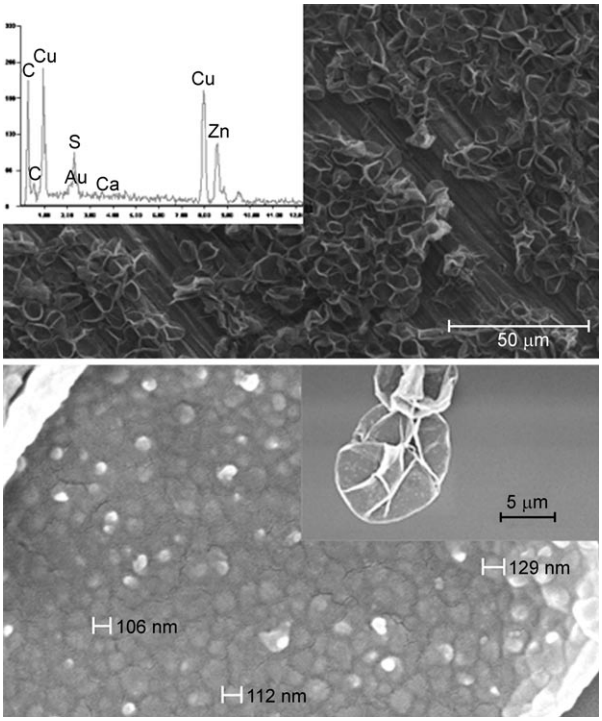

Figure 11. Top: FESEM-EDX analysis of collapsed hollow PE (PAH/PSS)$_6$ microcapsule samples on an alloy (Cu and Zn) platform. The inset shows EDX analysis of calcium ions. Bottom: FESEM image of some individual capsules. A low-magnification images is shown in inset, samples on mica. The templates for fabricating the capsules are from batch A.

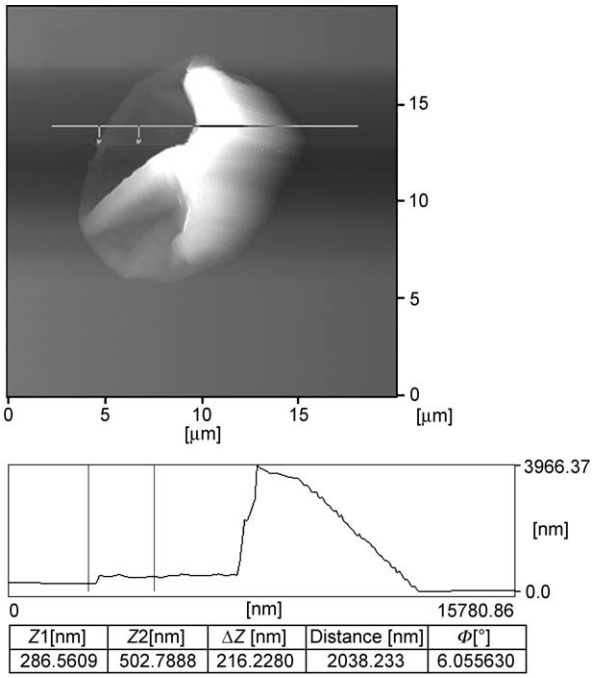

Z1[nm]	Z2[nm]	ΔZ [nm]	Distance [nm]	Φ[°]
286.5609	502.7888	216.2280	2038.233	6.055630

Figure 12. Top: AFM image of $(PAH/PSS)_6$ capsule from batch A. Bottom: thickness of the capsule wall ($\Delta H = \Delta Z/2$ nm). The templates for fabricating the capsules are from batch A.

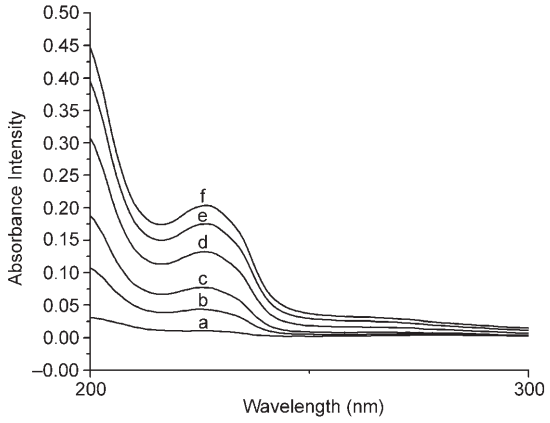

Figure 13. UV/Vis absorption spectra of $(PAH/PSS)_{1-5}$ multilayers and $\{(PAH/PSS)_5/PAH\}$/micelles formed by block copolymer on silica slides. a) One bilayer, b) two bilayers, c) three bilayers, d) four bilayers, e) five bilayers, f) $\{(PAH/PSS)_5/PAH\}$/PS-*b*-PAA.

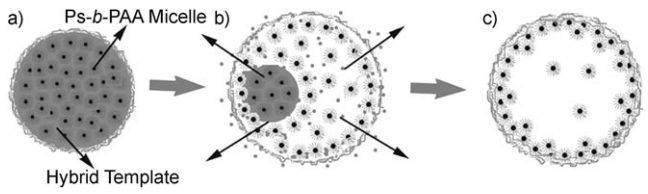

Scheme 2. Spontaneous-deposition mechanism based on the formation of the supramicelle congeries network during the core-dissolution process: a) polyelectrolyte-coated hybrid microparticles; b) core dissolution; c) formation of "micelles-enhanced" polyelectrolyte capsules.

sules were fabricated on the hybrid templates (Scheme 2a), templates were decomposed in trisodium-EDTA solution (b), and micelles-enhanced capsules were obtained (c).

Conclusion

Low dispersed hybrid $CaCO_3$ microparticles were synthesized in the presence of block copolymer PS-*b*-PAA. By modulating the concentration of block copolymer in the initial reaction system, the size of the hybrid microparticles can be easily controlled. Study of the mechanism of hybrid-particle formation revealed the acid-resistant properties of the hybrid microparticles. In addition, by adopting hybrid $CaCO_3$ microparticles as functional templates to fabricate PE capsules by the LBL technique, novel "micelles-enhanced" PE capsules were obtained. The permeability of the hybrid capsule wall should change as the capsule wall is reconstructed by negatively charged PS-*b*-PAA-based micelles. In addition, the presence of many stable and isolated micelles and/or micelle congeries leads to a huge negatively charged surface inside the capsule. All these factors inevitably have a great effect on the physicochemical properties of PE capsules, such as stability, encapsulation, and release behaviors for guest molecules. In contrast to conventional templates, this kind of template not only served as a physical support, but also afforded special properties to PE capsules. Consequently, the structure and properties of PE capsules can be tailored by designing different functional templates. We are continuing our studies of the encapsulation and release behaviors of these novel hybrid capsules.

Experimental Section

Materials: Amphiphilic block copolymer polystyrene-*b*-poly(acrylic acid) (PS-*b*-PAA) ($M_w = 12500$, molar ratio of PS:PAA was approximately 2.0) was obtained from Rohm and Hass. Poly(sodium styrenesulfonate) (PSS) ($M_w = 70$ kD) and poly(allylamine hydrochloride) (PAH) ($M_w = 70$ kD) were from Aldrich. FITC was purchased from Sigma. All other reagents were commercially available and were used as received.

Microparticle preparation: Preparation of hybrid calcium carbonate microparticles in the presence of block copolymer PS-*b*-PAA was performed according to the following method. Different amounts of PS-*b*-PAA were dissolved in 0.2 M sodium carbonate. $CaCl_2$ solution (2.0 M) was introduced to form a supersaturated calcium carbonate solution. The molar ratio of Na_2CO_3 to $CaCl_2$ was about 1:1. The progress of the reaction was inspected by optical microscopy. The reaction was ceased after 30 min at RT. The precipitate was rinsed thoroughly with deionized (DI) water by using the membrane filtration technique (0.8 μm membrane), then dried in a blowing oven at 50 °C, and eventually collected for testing. According to the initial concentration of PS-*b*-PAA in the reaction system (0.24, 0.64, 1.28 mM), the precipitate was called batch A, batch B, and batch C.

Fabrication of PSS/PAA multilayers on hybrid $CaCO_3$ templates: PAH and PSS were absorbed onto hybrid $CaCO_3$ microparticles from 2 mg mL^{-1} polyelectrolyte solutions in 0.5 M NaCl, the first layer being PAH. After 10 min of adsorption, the coating cores were centrifuged and rinsed three times with DI water. The oppositely charged polyelectrolyte was then added. Each adsorption step was followed by triple rinsing with DI water. After the adsorption of 12 layers, the hybrid cores were dis-

solved in trisodium-EDTA (pH 7.28, determined by pH meter) for 30 min with agitation. The capsules were centrifuged, and the supernatant was removed. The capsules were resuspended in fresh trisodium-EDTA. This washing procedure with trisodium-EDTA was repeated eight times; the resultant suspension of the formed microcapsules was washed four times with DI water and stored in the centrifuge tubes. For CLSM observation, microcapsules with fluorescently labeled walls were fabricated by using PAH—FITC, according to the same procedure.

Interaction between PS-*b*-PAA micelles and PAH layers: Hybrid $CaCO_3$ templates were dissolved in 1% trisodium-EDTA solution to give a solution mixture. Up to 11 layers of {(PAH/PSS)$_5$PAH} were autoassembled onto the silica slides (pretreated with a mixture of H_2SO_4/H_2O_2 (7:3) for 2 h). The silica slides were then immersed into the solution mixture for 30 min, rinsed with DI water three times, and dried at RT. The six slides of even numbers of layers were mounted in the UV/Vis spectrometer sample holder and absorption spectra were registered, as shown in Figure 13, by using an uncoated slide as a reference. Absorption of the slide with the sixth bilayer is stronger than that of the slide with the fifth bilayer. The results suggest that the block-copolymer micelles can interact with PAH to form polyelectrolyte complexes.

Measurements: The critical micelle concentration (CMC) of PS-*b*-PAA was determined by using a fluorescence technique with pyrene as the probe.[10] Briefly, a known amount of pyrene in acetone was added to each of a series of 10-mL vials and the acetone was evaporated. The final concentration of pyrene was 6.0×10^{-7} M. A total of 10 mL of various concentrations of copolymer in 0.1 M Na_2CO_3 were added to each vial and then heated at 50 °C for 10 h to equilibrate the pyrene and the micelles, and left to cool for 10 h at RT. Steady-state fluorescence spectra were measured by using an F-4500 fluorescence spectrophotometer (Hitachi High-Technologies Corp., Tokyo, Japan) with a slit width of 2.5 nm for both excitation and emission. For the fluorescence measurements, 1 mL of solution was placed in a 1.0-cm quartz cell. All spectra were run on air-equilibrated solutions. For excitation spectra, the emission wavelength was 390 nm. Spectra were accumulated with a scan speed of 240 nm min^{-1}. All experiments were carried out at 25 °C. The CMC was obtained from a plot of the concentration dependence of the I_{338}/I_{333} ratios. It was identified as the polymer concentration that intersected with a straight horizontal line drawn through the steepest part of the curve. The CMC obtained was approximately 0.006 g L^{-1}.

After the microparticles were dispersed in aqueous solution, particle size and size distribution were determined by using a coulter LS-230 laser particle-size analyzer (Miami, America). Dried microparticles samples were mounted on metal stubs by using double-sided adhesive tape. SEM was carried out by using a Stereoscan 260 (Cambridge, England) after a gold–palladium layer was sputtered by an E-1020 ion sputter for 120 s. TGA was conducted by using a TA Instrument SDT 2960. Samples were heated at 10 °C min^{-1} from RT to 1000 °C in a dynamic nitrogen atmosphere (flow rate = 70 mL min^{-1}). X-ray diffraction measurements were carried out by using a D/Max-2550 X-ray diffractometer, using Ni-filtered $Cu_{K\alpha}$ radiation (40 KV, 300 mA). Powder samples were mounted on a sample holder and were scanned in 0.02° steps from 5–90° (in 2θ) with 0.5 s per step. Transmission electron microscopy (TEM) was performed by using a JEM 1230 microscope operating at an acceleration voltage of 80 kV. Samples were deposited from aqueous solutions onto copper EM grids precoated with a thin film of Formvar. Water was allowed to evaporate from the grids at atmospheric pressure and RT. Confocal laser fluorescence micrographs (CLSM) were collected by using a Zeiss laser scanning system equipped with a 100× oil immersion and a 40× objective. Scanning force microscopy (SFM) images were recorded in air at 20–25 °C by using a Nanoscope III multimode scanning force microscope (tapping mode, Digital Instruments, Santa Barbara, CA). The samples were prepared by applying a drop of the capsule solution onto freshly cleaved mica.

Acknowledgement

This work was supported by the National Natural Science foundation of China (no. 50173023), the key National Natural Science Foundation of China (no. 50333020), and the National Basic Research Program of China (973 program, no. 2005CB623902). The author would like to thank Dr. Zhang Jianxiang and Prof. Chen Yiyong for their advice on this study. The author also would like to thank Prof. Adi Eisenberg for his constructive discussions.

[1] G. Decher, *Science* **1997**, *277*, 1232–1237.
[2] a) E. Donath, G. B. Sukhorukov, F. Caruso, S. A. Davis, H. Möhwald, *Angew. Chem.* **1998**, *110*, 2323–2327; *Angew. Chem. Int. Ed.* **1998**, *37*, 2201–2205; b) F. Caruso, R. A. Caruso, H. Möhwald, *Science* **1998**, *282*, 1111–1114.
[3] a) M. S. Wong, J. N. Cha, K. S. Choi, T. J. Deming, G. D. Stucky, *Nano Lett.* **2002**, *2*, 583–587; b) P. Jiang, J. F. Bertone, V. L. Colvin, *Science* **2001**, *291*, 453–457; c) N. G. Balabushevitch, G. B. Sukhorukov, N. A. Moroz, D. V. Volodkin, N. I. Larionova, E. Donath, H. Möhwald, *Biotechnol. Bioeng.* **2001**, *76*, 207–213; d) X. P. Qiu, S. Leporatti, E. Donath, H. Möhwald, *Langmuir* **2001**, *17*, 5375–5380; e) S. M. Marinakos, M. F. Anderson, J. A. Ryan, L. D. Martin, D. L. Feldheim, *J. Phys. Chem. B* **2001**, *105*, 8872–8876.
[4] a) C. Schuler, F. Caruso, *Biomacromolecules* **2001**, *2*, 921–926; b) E. Donath, S. Moya, B. Neu, G. B. Sukhorukov, R. Georgieva, A. Voigt, H. Baumler, H. Kiesewetter, H. Möhwald, *Chem. Eur. J.* **2002**, *8*, 5481–5485; c) M. K. Park, C. J. Xia, R. C. Advincula, P. Schutz, F. Caruso, *Langmuir* **2001**, *17*, 7670–7674; d) D. V. Volodkin, A. I. Petrov, M. Prevot, G. B. Sukhorukov, *Langmuir* **2004**, *20*, 3398–3406.
[5] C. S. Peyratout, L. Dähne, *Angew. Chem.* **2004**, *116*, 3850–3872; *Angew. Chem. Int. Ed.* **2004**, *43*, 3762–3783.
[6] a) D. V. Volodkin, N. I. Larionova, G. B. Sukhorukov, *Biomacromolecules* **2004**, *5*, 1962–1972; b) H. G. Zhu, E. W. Stein, Z. H. Lu, Y. M. Lvov, M. J. McShane, *Chem. Mater.* **2005**, *17*, 2323–2328.
[7] a) G. B. Sukhorukov, L. Dähne, J. Hartmann, E. Donath, H. Möhwald, *Adv. Mater.* **2000**, *12*, 112–115.
[8] K. Naka, Y. Chujo, *Chem. Mater.* **2001**, *13*, 3245–3259.
[9] a) H. Cölfen, *Macromol. Rapid Commun.* **2001**, *22*, 219–252; b) K. Naka, Y. Tanaka, Y. Chujo, Y. Ito, *Chem. Commun.* **1999**, 1931–1932; c) D. B. DeOliveira, R. A. Laursen, *J. Am. Chem. Soc.* **1997**, *119*, 10627–10631; d) H. Cölfen, L. Qi, *Chem. Eur. J.* **2001**, *7*, 106–116; e) H. Cölfen, M. Antonietti, *Langmuir* **1998**, *14*, 582–589.
[10] M. Wilhelm, C. L. Zhao, Y. Wang, R. Xu, M. A. Winnik, J. L. Mura, G. Riess, M. D. Croucher, *Macromolecules* **1991**, *24*, 1033–1040.
[11] a) L. F. Zhang, A. Eisenberg, *Science* **1995**, *268*, 1728–1731; b) L. F. Zhang, A. Eisenberg, *J. Am. Chem. Soc.* **1996**, *118*, 3168–3181; c) L. F. Zhang, A. Eisenberg, *Science* **1996**, *272*, 1777–1779.
[12] a) S. W. Wise, *Science* **1970**, *167*, 1486–1488; b) *Human Body Anatomy* (Ed.: Chinese Medical University), People Sanitation Publishing House, Beijing, **1982**, pp. 10–11; c) Q. L. Hu, X. D. Li, J. C. Shen, *Chin. J. Mater. Res.* **2003**, *17*, 337–340.
[13] a) J. H. Fendler, E. J. Fendler, *Catalysis in Micellar and Macromolecular Systems*, Academic Press, New York, **1975**, pp. 35–38; b) *Surfactant and Analytical Chemistry* (Ed.: W. B. Qi), Chinese Computation Publishing House, Beijing, **1979**, pp. 68–74.
[14] *Modern Physical Chemistry* (Ed.: Z. A. Zhu), Science Publishing House, Beijing, **2001**, pp. 172–173.
[15] I. Estrela-Lopis, S. Leporatti, S. Moya, A. Brandt, E. Donath, H. Möhwald, *Langmuir* **2002**, *18*, 7861–7866.

Received: March 12, 2006
Published online: May 19, 2006

